



# Tribological characteristics of one-process and two-process cylinder liner honed surfaces under reciprocating sliding conditions

Wieslaw Grabon, Pawel Pawlus\*, Jaroslaw Sep

Rzeszow University of Technology, Poland

## ARTICLE INFO

### Article history:

Received 29 August 2009

Received in revised form

1 February 2010

Accepted 3 February 2010

Available online 12 February 2010

### Keywords:

Two-process surface

Cylinder liner

Surface topography

## ABSTRACT

This paper reports an experimental study of the effect of surface texture on cylinder liner wear. This research is important because the conjunction between piston rings and cylinder liner is one of the major sources to frictional losses in internal combustion engines. Experiments were conducted on a reciprocating tester. Specimens were cut from cylinder liners honed or plateau honed made of grey cast iron of hardness 218 HB. The honing operation was performed in order to obtain very similar values of the  $Sq$  parameter of one-process and two-process surfaces. In addition, one-process specimens characterised by different  $Sq$  parameter values were tested. Counter-specimens were made from chromium-coated steel C45. It was found that wear of two-process surfaces was lower than that of one-process surfaces characterized by the same  $Sq$  parameter. Linear wear of specimens was proportional to initial  $Sq$  parameter value. The effect of additional oil pockets created by the burnishing technique on cylinder liner wear was negligible.

© 2010 Elsevier Ltd. All rights reserved.

## 1. Introduction

Cylinder liner, piston skirt, piston rings, valve train, crankshaft and its bearings are the major lubricated components in internal combustion engines. Major part of mechanical power loss in the engine is caused by friction in the piston-cylinder liner system. There are no doubts about the interest from both the manufacturers and customers in optimizing this mechanical system. Surface roughness of cylinder liners plays an important role in the control of tribological properties in the cylinder liner-piston ring system. Cylinder liner surface topography affects running-in duration, oil consumption, exhaust gases emission and engine performance.

Most engineering surfaces have height distributions which are approximately Gaussian. But multi-process textures are more important from a functional point of view. A plateau honed cylinder surface is the typical example of two-process texture. It contains traces of two processes: coarse honing and plateau honing. Honing is a process which is known to produce a Gaussian distribution of surface heights. A process of coarse honing followed by plateau honing will superimpose one Gaussian distribution on another. Plateau honed cylinder surface consists of smooth wear-resistant and load-bearing plateaux with intersecting deep valleys working as oil reservoirs and debris traps. Plateaued surfaces have been machined to simulate those that

result from normal running-in. At first, the recommended cylinder surface after one-process honing was very smooth. It showed high wear resistance during running-in. When surface roughness of cast iron cylinders increased ( $Ra=0.1-1.0\ \mu\text{m}$ ), their abrasive wear increased in co-action with chromium plated piston ring [1]. However, developments in engine design (mainly loading growth) led to increased incidence of scuffing failure for smooth liner surfaces. Only rough surfaces have a higher load-carrying capacity. Wiemann tested cylinder liners in internal combustion engine under conditions favourable to point seizure creation. He found that seizure resistance of cylinder liners without additional surface treatment is proportional to surface roughness height [2]. An excessive increase in the cylinder surface roughness amplitude (surfaces, for which  $Ra > 1\ \mu\text{m}$ ) is also detrimental; it causes an increase in chromium piston ring wear and an increase in engine oil consumption. The authors of paper [3] studied on internal combustion engine the effect of cylinder liner roughness height on the first piston (gas) ring wear, characterized by decrease of ring width. It was found that when the  $Ra$  parameter was in the range  $0.17-0.86\ \mu\text{m}$ , piston ring wear was small. When cylinder liner roughness height was higher, piston ring wear considerably increased. Running-in wear studies, conducted by the authors of Ref. [4] on a compression ignition engine showed that at top dead centre locations (outer returnable position) of piston rings the linear wear of the cylinder increased with increase in its initial surface roughness height, characterized by the  $Ra$  parameter in the range of  $0.2-0.5\ \mu\text{m}$ , but decreased with further increase of roughness amplitude from  $0.5$  to  $0.8\ \mu\text{m}$ . Because of great

\* Corresponding author. Tel.: +48 17 8651183; fax: +48 17 8651184.  
E-mail address: [ppawlus@prz.rzeszow.pl](mailto:ppawlus@prz.rzeszow.pl) (P. Pawlus).

tendency to seizure of smooth surfaces, an initial surface finish of the cylinder of  $0.8 \mu\text{m}$   $R_a$  was recommended.

Surface roughness after one process [1–4] is usually characterized by the  $R_a$  parameter.  $R_a$  is arithmetical mean deviation of the assessed roughness. This statistical parameter is commonly used by a majority of industrial firms to characterize roughness height of manufactured elements.  $R_q$ —root mean square deviation of the assessed roughness profile is parameter correlated with  $R_a$ . It is parameter of more statistical nature than  $R_a$ . Therefore, it is applied in theoretical investigations of friction, contact problems etc.

Scientists made efforts to find an optimum geometrical cylinder structure. A plateau-honed cylinder surface ensures simultaneously the sliding properties of a smooth surface and a great ability to maintain oil on a porous surface. It was found that plateau surfaces ensured shortening of the running-in time and lower wear in this period. These surfaces cannot be characterised by only one height parameter, as  $R_a$ . Material ratio curve is often used. This curve (the Abbott curve) is usually used to quantify wear phenomena such as lubricant influence, bearing materials or surface topography. It corresponds to  $1-f(x)$  where  $f(x)$  is the cumulative density function (the ordinate distribution) of surface height. The material ratio of the surface is the ratio of the sum of the surface elements at a given level to the evaluation length. Parameters  $R_p$  and  $R_v$  are connected with material ratio curve. Area under material ratio curve represents material volume (the  $R_v$  parameter), but above material ratio curve volume free of material (the  $R_p$  parameter).  $R_p$  is maximum roughness profile peak height,  $R_v$ —maximum profile valley depth. Total roughness profile height  $R_t$  is sum of  $R_p$  and  $R_v$ . The emptiness coefficient  $R_p/R_t$  (see Fig. 1a) describing asymmetry of the roughness profile (it is small for high profile asymmetry) is measure of contact deformation and wear resistance. For bearing surfaces small value of the emptiness coefficient is recommended. Surface after honing (one-process) of Gaussian ordinate distribution is characterised by  $R_p/R_t$  value about 0.5, however after plateau honing (two-process surface) by smaller  $R_p/R_t$  value. It is possible to discriminate surfaces after one and two processes on the basis of the cumulative distribution plot on normal probability graph. Material probability curve is a representation of the material ratio curve in which the profile material ratio is expressed as Gaussian probability in standard deviation values, plotted linearly on the horizontal axis. This scale is expressed in standard deviations. In this scale the material probability curve of a Gaussian distribution is a straight line. The slope of this line is the  $R_q$  parameter. For two-process surface composed of two Gaussian distributions, the material probability curve consists of two linear regions.  $R_p$  parameter is the slope of a linear regression performed through

the plateau region, but  $R_v$ —through the valley region. The intersection point  $R_{mq}$  defines the separation of plateau and base textures (ISO 13565-3 standard). Fig. 1b presents graphical interpretation of  $R_{pq}$ ,  $R_{vq}$  and  $R_{mq}$  parameters.

Campbell [5] compared theoretically wear of honed (one-process) and plateau honed (two-process) surfaces. They were characterised by the same roughness height and various shapes of the material ratio curve. Analysis indicated that to achieve a 30% material ratio in the running engine twice the volume of metal would be worn from a typical (one-process) surface than from a plateau surface. Pawlus [6] analysed the effect of surface topography of honed cylinders on their wear resistance during running-in. He found that the values of the local linear wear of cylinders having the same roughness height were proportional to the emptiness coefficient  $R_p/R_t$ . An increase in the initial roughness height also caused an increase in cylinder wear intensity.

The problem of running-in wear of cylinder liners seems to be very important. The surface remaining after this period is more gradually reduced and may last during long-term operation of the engine. Therefore, the influence of cylinder surface roughness on wear of piston-cylinder assemblies may exist not only in the initial period of engine life, but also in the case of large wear values. It was found that linear wear of cylinders under artificially increased dustiness abrasive conditions was proportional to the emptiness coefficient  $R_p/R_t$  and to distance between the deep valleys [7]. It was confirmed that  $R_p/R_t$  is a relevant parameter to characterize wear of cylinder (wear is smaller for lower values of this parameter [6,7]).

Tomanik [8] investigated, through reciprocating bench test, friction and wear of some new engine bore finishes, including structured laser ones. It was found that the structure with laser dimples of 3 mm long in circumferential direction and the smooth non-laser region showed the lowest friction. For the ring wear, the smoother variants caused lower wear. A textured surface combining the laser dimples on the top dead centre region and a very smooth finish along the rest of the stroke, may combine the lower friction advantage of the very smooth finish along the stroke with the oil reservoirs on the textured region. The authors of paper [9] modelled micro-scale abrasion in superfinishing belt grinding. Applications of a stochastic model in a mixed lubrication regime and of an optimization scheme allowed to obtain values of required roughness parameters. It was found that all two-process surfaces given by Tomanik [8] were in the specification given in article [9]. This analysis clearly validates the fact that specifications given by the automotive designer are well posed.

Jeng [10] compared one-process and two-process (plateaued) surfaces characterised by the same value of the  $R_q$  parameter using a pin-on disc tribometer. He found that in the mixed

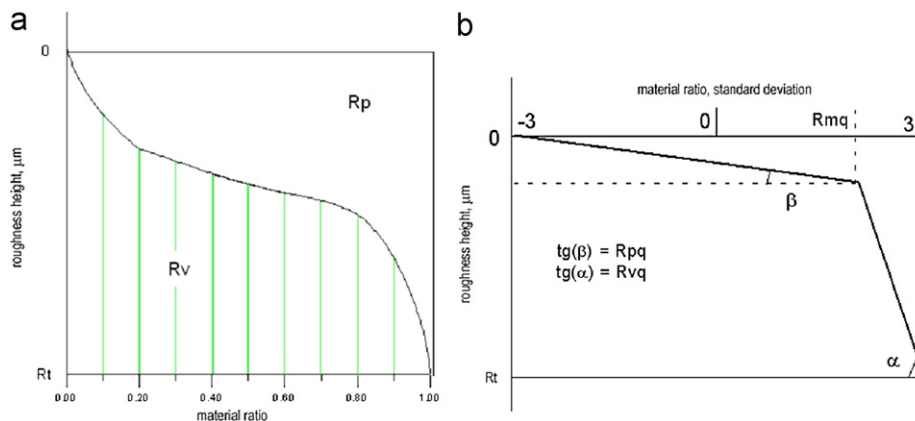


Fig. 1. Graphical interpretation of the  $R_p$ ,  $R_v$  and  $R_t$  parameters (a), the  $R_{pq}$ ,  $R_{vq}$  and  $R_{mq}$  parameters (b).

lubrication regime a plateaued surface presented less friction and higher wear resistance than a conventional surface of Gaussian ordinate distribution, probably because the  $Rpq$  parameter of two-process surface was smaller than the  $Rq$  parameter of one-process surface. However under condition of hydrodynamic lubrication the friction of samples with two analysed surfaces was similar.

It is difficult to find other studies comparing the tribological performance of one- and two-process surface topographies. However the evidence suggests two-process surfaces have advantages over conventional one-process surfaces.

When the wear amount is smaller than the initial surface height the wear intensity is usually proportional to roughness amplitude [11–13]. Two possible wear mechanisms can occur: wear removal due to abrasion (or adhesion) or plastic deformation (redistribution of material without net loss).

During the “zero-wear” process the wear volume or wear loss is within the limits of the original surface topography of the component. The local wear amount is then difficult to determine by common metrological methods. Therefore a surface profile measurement can be used to determine the amount of wear. Refs. [14–18] show examples of profilometric method applications for cylinder bore wear. Rosen et al. [14] believed that a practical problem of wear measurement was the difficulty of establishing a datum for changes in topography. They proposed the transition points (of abscissa  $Rmq$ ) between the two topographies of plateau honed surfaces as an absolute height datum for successive measurements. Daskivich [15] found that the highest point of the profile was real and was the contact point for a dimensional gauge-tip measurement of the bore diameter. He proposed the distance between the highest peak and a line intersecting the peaks such that half this line was in the metal (material ratio of 0.5). Pawlus [16] found that it was possible to measure “zero-wear” value of cylinder liners using changes in profile parameters.  $Rt$ ,  $Rtm$ ,  $Rz$  and  $R3z$  were proposed, of which  $Rtm$  was recommended.  $Rtm$  is arithmetical mean of the highest roughness profile height within 5 sampling lengths,  $Rz$  is ten-point height of the roughness profile and  $R3z$  is arithmetical mean of vertical distance between the third highest peak and the third deepest valley within 5 sampling lengths. The variability of the recommended  $Rtm$  parameter on cylinder surface is small, changes of this parameter are correlated and similar to cylinder liner radial wear measured by bar gauge (for small liner distortion). The authors of paper [17] proposed a new procedure to evaluate cylinder liner wear volume and depth under a “zero-wear” regime. It was considered that 90% of the material ratio curve was the same before and after wear. The material ratio curve of the worn liner was transformed by the depth differences at 90% and the area between the two curves (of original and used liners) representing the material worn from the profiles parallel to the cylinder axis was calculated. The wear depth was obtained by the projection of the 30–70% line on the depth axis of two material ratio curves and then finding their difference. This method was considered superior to gauging the changes in diameter (such determination is influenced by the cylinder liner distortion). The authors of paper [18] estimated the amount of volumetric wear from measurement of the surface profile before and after “zero-wear” as the difference of material ratio curves. Such methods require a relocation technique to find the same area for comparison and very precise positioning of the 3D measurement area before and after the wear test. Then the lateral matching of the two images is necessary. Unworn elements (for example the deepest valleys) may be used as Refs. [19,20]. Cross-correlation functions can be used for proper matching [21]. It is also possible to estimate wear without measuring the initial surface topography when unworn elements exist on the surface.

The fundamental aim of this study is to directly compare the tribological performance of one-process and two-process cylinder

liner surfaces, characterised by the same value of the  $Sq$  parameter, under a controllable test environment. The other purposes are to recommend the method of obtaining the local linear wear of a cylinder liner on the basis of profilometric measurement, to study connection between initial value of the  $Sq$  parameter and the liner linear wear as well as to analyse the changes in the liner surface topography.  $Sq$  is the 3D extension of the  $Rq$  roughness profile parameter.

## 2. Experimental

### 2.1. Tribological tester and operating conditions

The experiments were conducted on a reciprocating tester (see Fig. 2).

In the tribological tester the rotational movement was changed into reciprocating movement by a crankshaft assembly. The drive from an electric motor through a V-belt transmission (transmission ratio 1:2) was transmitted to the crankshaft. The radius of the crank was 45 mm, so its stroke was 90 mm. The machine is equipped with sensors of normal and friction forces CL14 of range 2KN from the ZEPWN firm (the error of measurement was 0.25% of the measuring range) and with a system of oil lubrication assuring the temperature of oil in reservoir about 80 °C. Temperature of the oil supplied to the sliding pair was about 40 °C. The lubricant used was SUPEROL SAE CB 40 oil. It was supplied into the inlet side of the contact zone.

In order to speed adjustment frequency converter in conjunction with a three-phase induction motor made by the TAMEL firm was used. The rotational speed can be changed from 0 to 2850 rev/min. The design of the tribological tester allows us to easily change the operating parameters for example; normal force or velocity and the tested elements can be quickly replaced.

A special fixing was designed and made for friction pair. The counter-specimen (2) is articulated on a ball-and-socket joint (4) of a mandrel (3)—see Fig. 2. This construction allows an intimate contact of samples from cylinder liner and piston ring during reciprocation.

The results of friction force measurement were recorded using the laboratory measuring system DaqLab 2000. During tests the temperature of the sample was continuously measured in four places by a thermometer with resistance temperature sensors (measuring uncertainty  $\pm 0.4$  °C).

The operating parameters were as follows:

- sliding velocity: 0.44m/s,
- unitary pressure: 8.3 MPa,
- frequency of lubrication: 0.0012 dm<sup>3</sup>/h,
- sliding distance: 6480 m (test duration 4 h).

Each test was repeated 3 times.

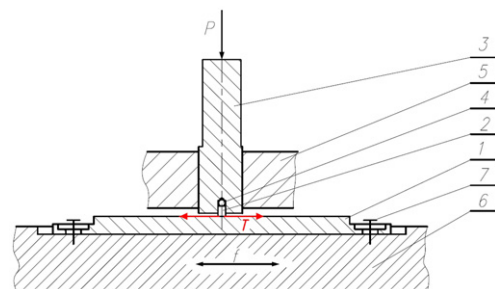


Fig. 2. The scheme of tested assembly: 1—specimen (cylinder liner detail), 2—counter-specimen (fragment of piston ring), 3—mandrel, 4—ball-and-socket joint, 5—frame, 6—shifted slide, 7—specimen clamping, P—force pressing down specimen, f—direction of slide movement, T—friction force.

The cylinder liner wear was within the limit of the original surface topography, so the local wear amount was difficult to determine. Therefore measurement of local microscopic wear was done using a 3D surface topography measuring equipment Talyscan 150 (the height resolution was about 10 nm). The measurement was done before and after the test in the same places. The measured area before the test was 4 mm × 4 mm (sampling interval in perpendicular directions was 5 μm). In order to measure the cylinder liner surface in exactly the same place before and after wear a relocation method (mechanical using Vicker's indenter and then digital) was used. After relocation, the areas where the parameters were calculated were smaller: 1 mm (axial direction) × 4 mm (circumferential direction). In order to obtain from the 3D measurement data of worn surfaces, profiles orthogonal to ring movement containing details subjected and not subjected to wear, measured area after the test was: 1 mm × 11 mm. In addition, after 0.5, 1, 2, 3 and 4 h of the test surface replicas from DURACRYL were made on cylinder liner details in order to assess wear intensity. DURACRYL® PLUS is acrylate chemo-hardenable material consisted from liquid and powder. After relocation, before parameters calculation a third-degree polynomial was fitted to the measurement data, digital filters were not used. We analysed the changes of some 3D surface topography parameters (defined in Table 1). Definitions of the majority of them are given in Ref. [22]. Parameters  $Spq$ ,  $Svq$  and  $Smq$  are the extensions of roughness parameters defined in ISO 13565-3 standard. They were calculated using the original software of the present authors. The procedure from ISO standard was applied, however different formula of conical curve approximating probability plots of material ratio curve was used.

Mass of counter-specimens was assessed using a laboratory balance LB-1050/2 of measuring uncertainty  $\pm 0.001$  g (measure-

ments in three places). The measurements were done at the beginning and at the end of each test.

## 2.2. Preparation of specimens

Grey cast iron cylinder liners of hardness 218 HB were taken as workpieces. This material is typically used in Diesel engines for heavy commercial vehicles. After boring, the plateau-honed surfaces were produced, employing diamond honing sticks (NAGEL Maschinen- und Werkzeugfabrik GmbH) in the rough honing process. The first stage of the process removes sufficient material to improve the cylindricity of the bore. After rough honing, using honing sticks of grit size of D151, the cylinder liner diameter was  $\varnothing 130.93 \pm 0.005 / -0.010$  mm, and the surface roughness  $Rz$  parameter was 19 μm. Experiments were then carried out on a vertical honing machine (Gehring Technologies GmbH). The first batch of cylinders (after one process) was subjected only to coarse honing using honing stones with a ceramic binder. The second batch of cylinder liners (after two processes) was coarse honed and plateau honed using sticks with a ceramic binder. The third batch of cylinder liners was subjected to coarse honing, impulsive burnishing (a special tool acted as a hammer to form dimples on the cylinder liner surface) and then plateau honing. During honing stones with ceramic binder were used. A honing oil (HON 15) especially designed for the honing process was allowed to flow into the honing zone during the process. The honing angle was about 50°.

Specimens were cut from these cylinder liners (see Fig. 3). The honing operation was performed in order to obtain very similar values of the  $Sq$  parameter for one-process and two-process surfaces: 0.4, 0.7 and 1.0 μm. In addition, two one-process specimens characterised by  $Sq$  parameter values of 0.2 and 1.8 μm were tested. Three further two-process surfaces characterised by  $Sq$  values of 0.4 and 0.8 μm had also oil pockets, created by the burnishing technique. Fig. 4 presents photos of surfaces contained dimples after wear process. The oil pockets were oriented with their shorter dimension in the sliding direction.

Tables 2 and 3 present the average values of parameters characterising the surface topography of the specimen used. These parameters were selected previously taking a correlation and regression analysis into consideration [23]. Samples K1M, K2B and K3VB contain the oil pockets created by burnishing (embossing) technique. Table 4 includes dimensions of these dimples: depth  $d$ , length  $l$ , width  $w$  and pit-area ratios  $S_p$ . Surface topography parameters of these samples were obtained in areas free of oil pockets.

## 2.3. Preparation of counter-specimens

Counter-specimens were made from steel C45. The working surface of the piston ring was chromium coated by electroplating. Then the ring was subjected to grinding for the outer diameter

**Table 1**  
Description of 3D surface topography parameters.

Parameter	Description
$Sa$	Arithmetical mean deviation of the surface
$Sq$	Root-mean-square deviation of the surface
$Sv$	Maximum depth of valleys
$Sp$	Maximum height of summits
$St$	Total height of the surface
$Sz$	Ten-point height of the surface
$SHtp$	Surface section height difference corresponding to 20–80% of the material ratio
$S\Delta Htp$	Surface section height difference corresponding to 5–95% of the material ratio
$Sk$	Core depth
$Spk$	Reduced summit height
$Svk$	Reduced valley depth
$Sr1$	Material ratio of summits
$Sr2$	Material ratio of valleys
$Ssk$	Skewness of the surface
$Sku$	Kurtosis of the surface
$S\Delta q$	Root-mean slope of the surface
$Ssc$	Arithmetic mean summit curvature of the surface
$Sdr$	Developed interfacial area ratio
$Str$	Texture aspect ratio of the surface
$Sal$	Fastest decay autocorrelation length
$Sds$	Density of summits of the surface
$Std$	Texture direction
$Sbi$	Surface bearing index
$Sci$	Core fluid retention index
$Svi$	Valley fluid retention index
$Spq$	Plateau standard deviation
$Svq$	Valley standard deviation
$Smq$	Material ratio in intersection between plateau and valley textures

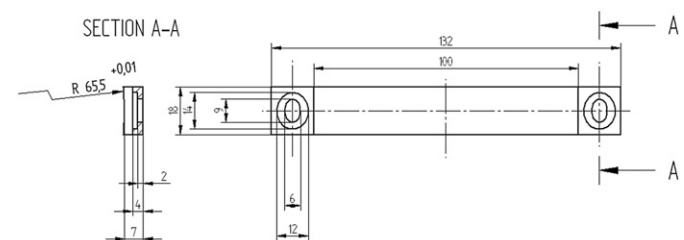


**Fig. 3.** Shape and dimensions of specimen.

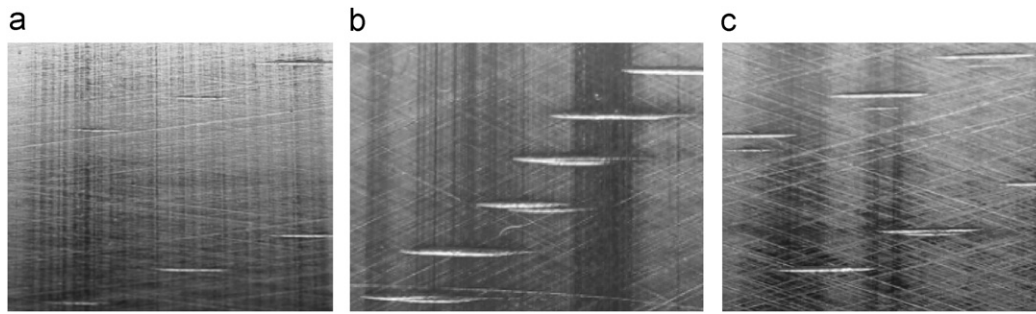


Fig. 4. Photos of surfaces with burnished oil pockets: (a) K1M, (b) K2B, (c) K3VB. Pictures were taken after the test.

Table 2

Average values of surface topography parameters of one-process surfaces.

Specimen designation	Parameters									
	Sq ( $\mu\text{m}$ )	Sz ( $\mu\text{m}$ )	Ssk	Sal (mm)	Std (deg)	Str	Ssc ( $\mu\text{m}^{-1}$ )	Sk ( $\mu\text{m}$ )	Svk ( $\mu\text{m}$ )	Sr2 (%)
I-0.2	0.21	1.41	-0.49	0.0081	25.5	0.121	0.0069	0.237	0.141	87.2
I-0.4	0.37	3.04	-0.85	0.0152	26.0	0.053	0.0113	0.731	0.523	84.7
I-0.7	0.72	10.7	0.83	0.0087	25	0.0673	0.0394	1.58	0.83	88.9
I-1.0	0.99	8.84	-0.41	0.0049	26.5	0.028	0.0441	2.06	1.26	88.3
I-1.8	1.77	16.3	0.21	0.0021	25.0	0.177	0.071	4.09	2.06	87.1

Table 3

Average values of surface topography parameters of two-process surfaces.

Specimen designation	Parameters												
	Sq ( $\mu\text{m}$ )	Sz ( $\mu\text{m}$ )	Ssk	Sal (mm)	Std (deg)	Str	Ssc ( $\mu\text{m}^{-1}$ )	Sk ( $\mu\text{m}$ )	Svk ( $\mu\text{m}$ )	Sr2 (%)	Spq ( $\mu\text{m}$ )	Svq ( $\mu\text{m}$ )	Smq (%)
II-0.4	0.41	8.03	-2.3	0.0067	26.5	0.052	0.027	0.545	0.904	84.1	0.186	1.761	91.94
II-0.7	0.739	6.04	-1.4	0.0085	26.5	0.047	0.033	1.44	1.29	79.2	0.358	1.622	72.1
II-1.0	1.01	10.3	-1.1	0.0059	26.5	0.053	0.046	2.55	1.51	84.1	0.348	1.732	60.66
K1M	0.351	3.93	-1.7	0.0026	25.5	0.131	0.026	0.71	0.76	87.5	0.211	0.829	95.85
K2B	0.392	4.14	-2.5	0.0028	25.0	0.071	0.021	0.441	0.973	81.5	0.155	1.516	86.51
K3VB	0.823	7.07	-1.2	0.0018	25.5	0.036	0.035	1.71	1.25	85.5	0.621	1.499	78.61

Table 4

Characteristics of oil pockets.

Specimen designation	d ( $\mu\text{m}$ )	l ( $\mu\text{m}$ )	w ( $\mu\text{m}$ )	S <sub>p</sub> (%)
K1M	12	1320	109	0.8
K2B	15	2370	126	1.7
K3VB	25	2410	128	1.8

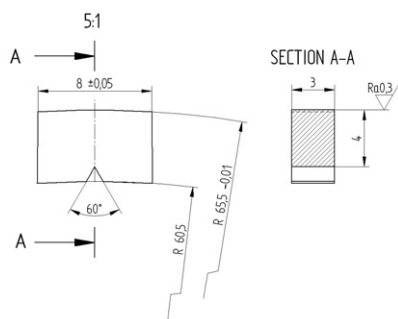


Fig. 5. Shape and dimensions of counter-specimen.

Ø 131–0.02 mm. Counter-specimens (see Fig. 5) were cut from these rings. Micro-hardness of the coating was 835 HV1/10 (the roughness Ra parameter was 0.3  $\mu\text{m}$ ).

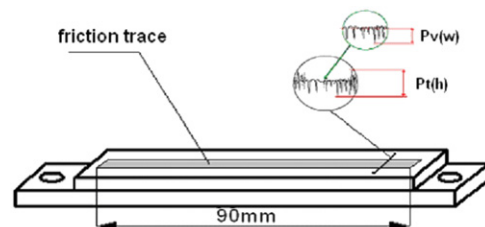


Fig. 6. The method of measurement of ZPr.

### 3. Results and discussions

#### 3.1. Assessment of the cylinder liner local wear

From the 3D measurement data we obtained a profile orthogonal to ring movement and to wear traces (see Fig. 6). This profile contains details subjected and not subjected to wear. In order to avoid errors, the profile obtained from the raw surface was only leveled. In order to obtain the wear it was necessary to analyse the middle profile fragment without the profile details not subjected to wear. The  $Pv(w)$  parameter (maximum valley depth) of this profile zone was obtained. The average wear called ZPr is equal to the  $Pt(h)$  parameter (total profile height) of the whole profile minus the  $Pv(w)$  parameter of the middle fragment. Therefore the linear wear is the difference between the highest point of profile detail of the unworn surface and the mean line of

profile detail of the worn surface. Because of repetitions of profiles measurement (6) we obtained average linear wear values. A similar procedure was used in Ref. [24]. Fig. 7 presents example of ZPr parameter obtained.

It is not always possible to obtain linear wear based only on the measurement of worn surface topographies because the reference elements (unworn surface details) do not exist. Therefore finding a method of wear measurement based on changes of surface topography parameters during wear is a problem of great practical importance; it can be used during measurement of real cylinders. Changes of height parameters can be taken as local wear measures. Based on the analysis of parameter changes we recommend parameters which decreased during wear (in all the analysed cases). We proposed to use the following parameters: *Sp*, *Spk*, *Sk* and *SHTp*. The other parameters, like the parameter recommended by Kumar et al. [17], the height corresponding to material ratio 0.13–99.87% [25] or 5–95% ( $\Delta Htp$ ) [24] sometimes increased during wear. Fig. 8 presents the dependence between selected parameters changes and average values ZPr of the tested samples. The regression equations and the coefficients of determination (square of the linear correlation coefficient) are also presented. It is evident from Fig. 8 that one can obtain wear amounts based on changes in the *Sk* parameter. The values of the linear correlation coefficient *R* between changes in the *Spk* and *SHTp* parameters and wear measure ZPr are a little smaller. The application of the change of *Sp* parameter as the local linear wear measures is not recommended.

3.2. Connection between initial cylinder liner surface topography and its linear wear

Table 5 presents the results of ZPr measurement. Fig. 9 presents connections between the *Sq* parameter values of

**Table 5**  
Average values and measuring uncertainties of the linear wear ZPr.

Specimen designation	Linear wear ZPr	
	Average value (μm)	Uncertainty (μm)
I-0.2	0.95	0.2
I-0.4	1.19	0.24
I-0.7	2.31	0.31
I-1.0	2.65	0.32
I-1.8	6.36	0.26
II-0.4	1.11	0.35
II-0.7	1.85	0.38
II-1.0	2.28	0.24
K1M	1.04	0.1
K2B	1.14	0.4
K3VB	2.39	0.44

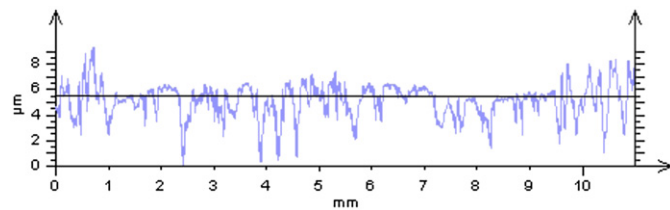


Fig. 7. Example of determination of linear wear of sample I-1.8 (ZPr=4.39 μm).

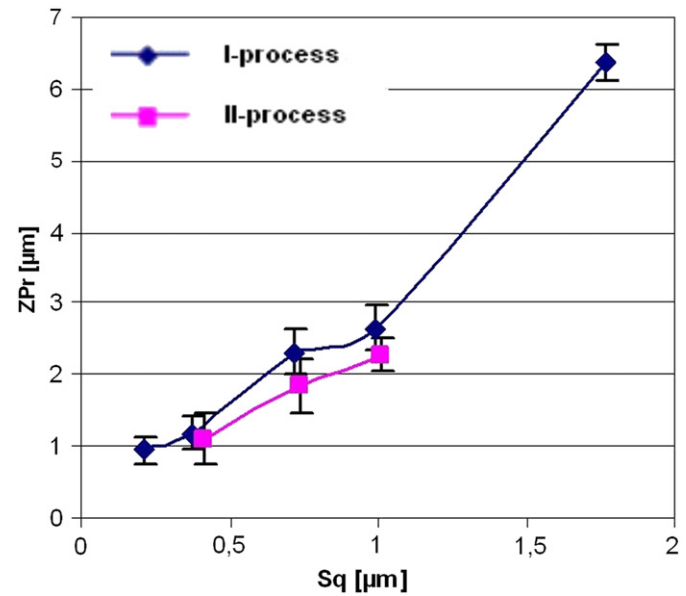


Fig. 9. Connection between initial value of the *Sq* parameter and the linear wear ZPr of honed and plateau honed surfaces.

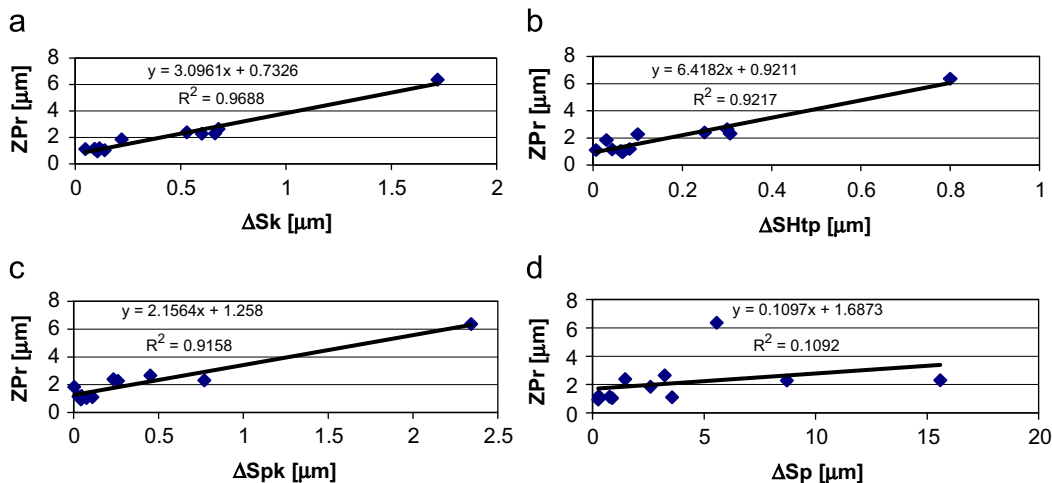


Fig. 8. Dependencies between  $\Delta Sk$ ,  $\Delta Spk$ ,  $\Delta SHTp$ ,  $\Delta Sp$  and the wear measure ZPr.

surfaces after one- and two-processes (samples having oil pockets created by burnishing technique were excluded).

From the analysis of Fig. 9 one can see that wear of samples is higher for larger initial values of the  $Sq$  parameter. Wear of specimens after two processes is smaller than wear of one-process samples, the surface topography of which is characterised by the same initial value of the  $Sq$  parameter. The difference is small for the  $Sq$  parameter of  $0.4\ \mu\text{m}$ , but higher for larger surface height, however the scatter range was partially coincident. When the  $Sq$  parameter value of the one-process surface (I-0.2) was similar to the  $Sq$  parameter value of the surface after two processes (II-0.4), linear wear of samples II-0.4 was greater, however the difference was not statistically important. Specimens with two-process surfaces (II-0.4 and II-0.7) of the  $Svq$  parameter similar to the parameter  $Sq$  of the one-process sample I-1.0 were characterized by much smaller wear.

The influence of additional oil pockets created by the burnishing technique on cylinder wear was not substantial. From among samples having oil pockets created by the impulsive burnishing technique K3VB was the worst, but K1M (of dimensions the most similar to the requirement of leading engine builders) was the best taking linear wear value into consideration. It seems that surface topography between oil pockets has an influence on cylinder wear (see Tables 2–5).

We analysed also dependencies between initial surface topography parameters and cylinder liner linear wear  $ZPr$ . It was not possible to find a correlation between initial values of parameters characterizing the shape of the surface topography ordinate distribution, spacing parameters, mean summit curvatures and linear wear  $ZPr$ . Fig. 10 presents the most important connections found. Dependencies are rather strong (the coefficient of determination  $R^2$  is greater than 0.94). Therefore wear is larger when the initial values of the amplitude parameters  $Sk$ ,  $Sq$  and  $SHTp$  as well as rms. slope  $S\Delta q$  are higher. When the linear correlation coefficients were used, they were the biggest when the parameters  $Sq$  and  $Sk$  were used ( $R$  was higher than 0.94). We also analysed the results of an investigation when multiple regression method was applied. There were the following input parameters:  $Sq$ ,  $Ssk$ ,  $Sal$ ,  $Std$ ,  $Str$ ,  $Ssc$ ,  $Sr2$  and  $Sz$ . The only statistically important dependence was found between  $Sq$  and  $ZPr$ . Similar connections were obtained when the  $Sq$  parameter was changed into parameters shown in Fig. 10:  $Sk$ ,  $SHTp$  and  $S\Delta q$  (these parameters were correlated with  $Sq$ ).

Wear intensity was studied from the analysis of surface replicas. It is evident that wear intensity decreases when sliding distance  $L$  is greater than 0.8–1.6 km (see Fig. 11). Values of mass wear of counter-specimens were similar (about 0.002 g).

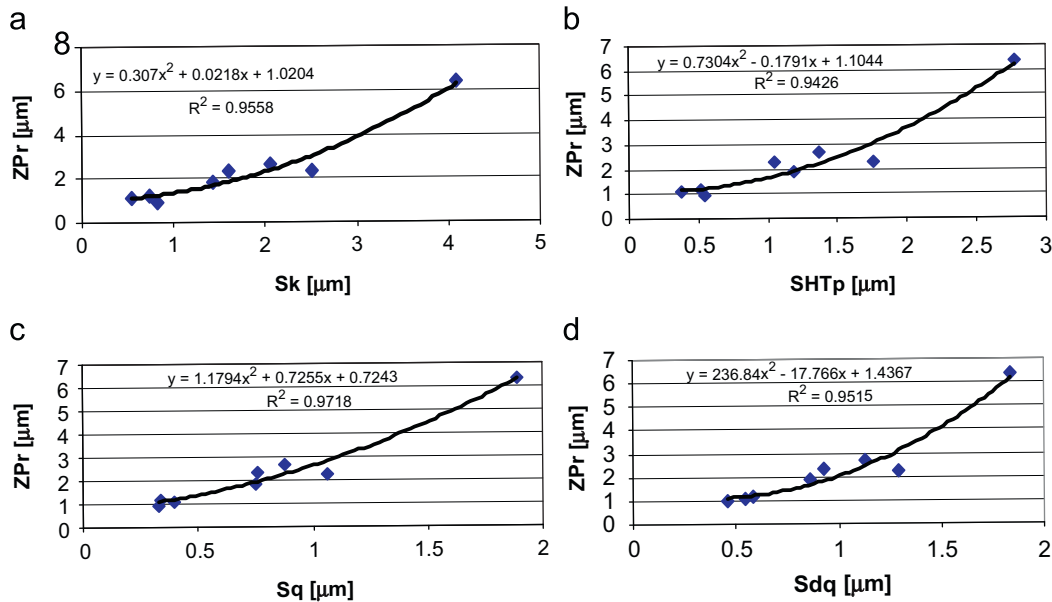


Fig. 10. Dependencies between initial values of parameters  $Sk$ ,  $SHTp$ ,  $Sq$ ,  $S\Delta q$  ( $Sdq$ ) and the linear wear  $ZPr$ .

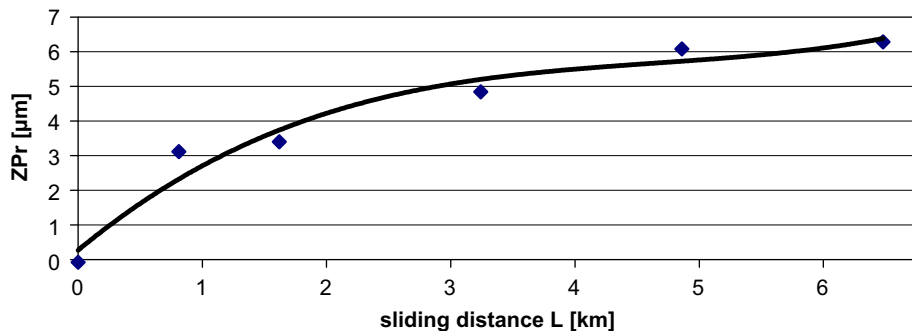


Fig. 11. Linear wear of cylinder liner I-1.8 versus sliding distance.

3.3. Connection between initial cylinder liner surface topography and coefficient of friction of tested assembly

The connection between initial surface topography of cylinder liners characterised by the *Sq* parameter value and the coefficient of friction was studied. Table 6 presents the values of the coefficient of friction obtained during wear resistance tests (4 h). The effect of the number of processes on the coefficient of friction was negligible although values of the coefficient of friction of two-process surfaces were a little smaller than those values corresponding to two-process surfaces with the same initial value of the *Sq* parameter. One can see an optimum range of *Sq* parameter (0.4–0.7 μm), for which the coefficient of friction obtained a minimum value. The substantial influence of dimples creation by the burnishing technique on the coefficient of friction was not confirmed, however the average value of the coefficient of friction with sample K1M was a little higher than that for sample I-0.4 with a similar value of the *Sq* parameter. The high scatter of results proves the necessity of further modification of tribological tester.

The values of coefficient of friction usually decreased during the wear process (see Fig. 12); which proves good accommodation of the sliding surfaces. Reduction of friction during the test was also observed by Tomanik [8].

3.4. Change of cylinder liner surface topography during wear

3.4.1. Changes of one-process surfaces

At first we analysed changes in surface topography of one-process surfaces. Table 7 presents relative changes of selected surface topography parameters with the same tendency of changes.

Some height parameters decreased during “zero-wear”. The changes of statistical parameters (*Sa*, *Sq*), *SHtp* and *SΔHtp* were

smaller than those of parameters describing the core (*Sk*) or peak surface part. Parameters describing material ratios *Sr1* and *Sr2* decreased during wear. During the “zero-wear” process the tendency of *Sku* increase was observed. The *Ssk* parameter is not presented in Table 7 (the relative changes were not calculated because of its initial value close to 0). In all the analysed cases the *Sal* spacing parameter increased (the changes were high). The slope *SΔq*, mean summit curvature *Ssc* and developed area *Sdr* decreased during wear. The changes were caused by an increase in the spatial parameter *Sal* and by the roughness height decrease. The change in the *Ssc* parameter was high because changes in parameters describing the peak surface part were large. The functional parameter *Sbi* increased during wear. Changes were high, which is connected with the decrease in *Sp* and *Spk* parameters (generally with high changes of a peak surface part). The *Sci* parameter decreased, but *Svi* increased during wear.

During the “zero-wear” process a two-process structure is created. The possibility of obtaining an *Spq* parameter value (0.15–0.28 μm) proves it (see Fig. 13). The tendency was found that a higher value of roughness height (characterised for example by the *Sk* parameter) corresponds to a larger value of *Spq* (see Fig. 14). The following range of the *Smq* parameter of worn surface was found: 43–89%, however for *Svq*: 0.98–1.66 μm.

The great changes of the majority of parameters took place during 0.5 and 1 h of operating (sliding distance *L* 0.8–1.6 km). The parameters connected with the peak surface part *Sp*, *Spk*, *Sr1* and *Ssc* changed mostly in the beginning of wear. However changes of parameters *SΔq*, *Sdr*, *Sci* and *Svi* were comparatively low.

3.4.2. Changes of two-process surfaces

Changes of two-process surfaces: II-0.4, II-0.7, II-1.0 and surfaces with burnished oil pockets (details of surface without

Table 6 Average values and measuring uncertainties of the coefficient of friction.

Specimen designation	Coefficient of friction $\mu$	
	Average value	Uncertainty
I-0.2	0.081	0.016
I-0.4	0.074	0.02
I-0.7	0.077	0.022
I-1.0	0.084	0.004
I-1.8	0.088	0.01
II-0.4	0.085	0.01
II-0.7	0.081	0.007
II-1.0	0.095	0.02
K1M	0.094	0.002
K2B	0.086	0.004
K3VB	0.085	0.004

Table 7 Absolute values of relative changes in selected surface topography parameters of one-process surfaces during wear.

Parameter	Average value (%)	Range (%)
<i>Sa</i>	21.2	11.2–32.1
<i>Sq</i>	21.5	7.8–34.2
<i>Sp</i>	62.9	28.1–92.3
<i>SHtp</i>	24.5	17.1–29.2
<i>SΔHtp</i>	22.1	11.2–37.3
<i>Spk</i>	65.8	24.1–90.2
<i>Sk</i>	36.5	15.2–48.4
<i>Sr1</i>	62.1	0.5–76.3
<i>Sr2</i>	7.5	0.6–11.2
<i>Sku</i>	56.0	20.3–85.1
<i>Sal</i>	508	166–946
<i>SΔq</i>	20.9	13.2–34.1
<i>Sdr</i>	35.1	22.1–55.6
<i>Ssc</i>	65.1	28.1–78.6
<i>Sbi</i>	467	56.1–1400.2
<i>Sci</i>	20.5	9.4–30.2
<i>Svi</i>	35.5	13.1–68.2

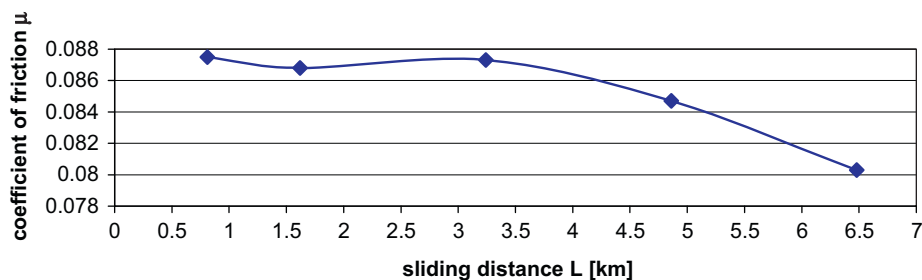


Fig. 12. The coefficient of friction versus sliding distance for assembly with sample K3VB.



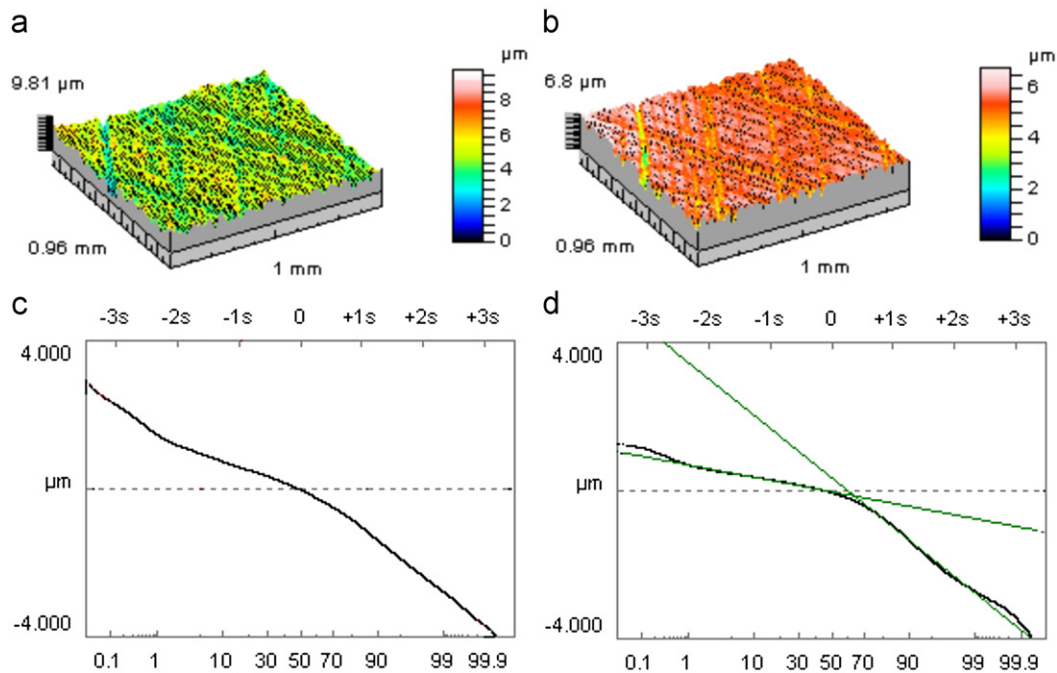


Fig. 13. Contour plots of surface details (a, b) and probability plots of material ratio curve (c, d) of I-1.0 sample before (a, c) and after test (b, d).

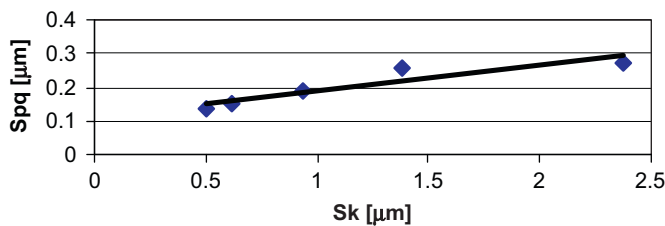


Fig. 14. Dependence between  $Sk$  and  $Spq$  parameters of worn one-process surfaces.

Table 8

Absolute values of relative changes in selected surface topography parameters of two-process surfaces during wear.

Parameter	Average value (%)	Range (%)
$Sp$	64.2	10.2–85.4
$SHTp$	8.9	0.7–24.3
$Spk$	31.2	5.1–55.4
$Sk$	16.6	3.5–41.5
$Sr2$	5.1	0.9–9.2
$Sku$	60.0	28.1–81.2
$Sds$	33.6	16.1–55.3
$Sal$	526	156–1100
$Ssc$	67.8	61.2–76.5
$Sbi$	598	16.1–1640.1
$Sci$	22.4	3.2–35.1
$Svi$	20.1	12.1–29.3
$Spq$	42.3	24.1–48.2
$Smq$	67.1	8.1–168

dimples) were analysed. Table 8 presents relative changes of surface topography parameters with the same tendencies. Differently from one-process surfaces, a not synonymous trend of statistical parameters  $Sa$  and  $Sq$  changes was noticed. However changes of these parameters were low (not higher than 21%). Parameters describing the roughness core  $Sk$  and  $SHTp$  and

parameters describing the peak surface part  $Sp$  and  $Spk$  decreased during wear, however changes of parameters  $Sp$  and  $Spk$  were large. Similarly to the one-process surfaces,  $Sr2$  decreased,  $Ssk$  decreased,  $Sku$  increased,  $Sal$  increased,  $Ssc$  decreased and  $Sbi$  increased. The  $Sci$  parameter decreased, but  $Svi$  increased. Differently from one-process surfaces the summit density  $Sds$  decreased during wear (see Table 8).

Probability parameter  $Spq$  decreased, but  $Smq$  increased during wear. It proves that the structure created during wear is still a two-process structure (see Fig. 15), the plateau structure created during plateau honing was removed. The  $Spq$  parameter is proportional to amplitude parameters, like  $Sk$  (see Fig. 16).

Similarly to changes of one-process surfaces, the biggest parameters changes were noticed after 0.5–1 h of operating. The largest changes were found in parameters characterizing the peak surface part  $Sp$ ,  $Spk$ ,  $Sds$ ,  $Ssc$  and  $Spq$ . Changes of parameters  $Sr2$ ,  $Sci$  and  $Smq$  were the smallest.

Generally, changes of parameters of initial surfaces after two processes were similar to those of the one-process surfaces. Decreases of amplitude parameters of two-process surfaces were smaller.

#### 4. Conclusions

- (1) It was found that wear of two-process surfaces was lower than that of one-process surfaces characterized by the same  $Sq$  parameter. Linear wear of specimens is proportional to initial values of the following parameters:  $Sk$ ,  $Sq$ ,  $SHTp$  and  $S\Delta q$ . The effect on cylinder liner wear of additional oil pockets created by a burnishing technique was negligible. The surface topography without oil pockets has an influence on cylinder wear. Wear intensity decreased constantly for sliding distances larger than 1.6 km.
- (2) The effect of the number of processes on the coefficient of friction is small. We found optimum values of the  $Sq$  parameter (0.4–0.7  $\mu\text{m}$ ), for which the coefficient of friction reached a minimum value. The high scatter of results proves

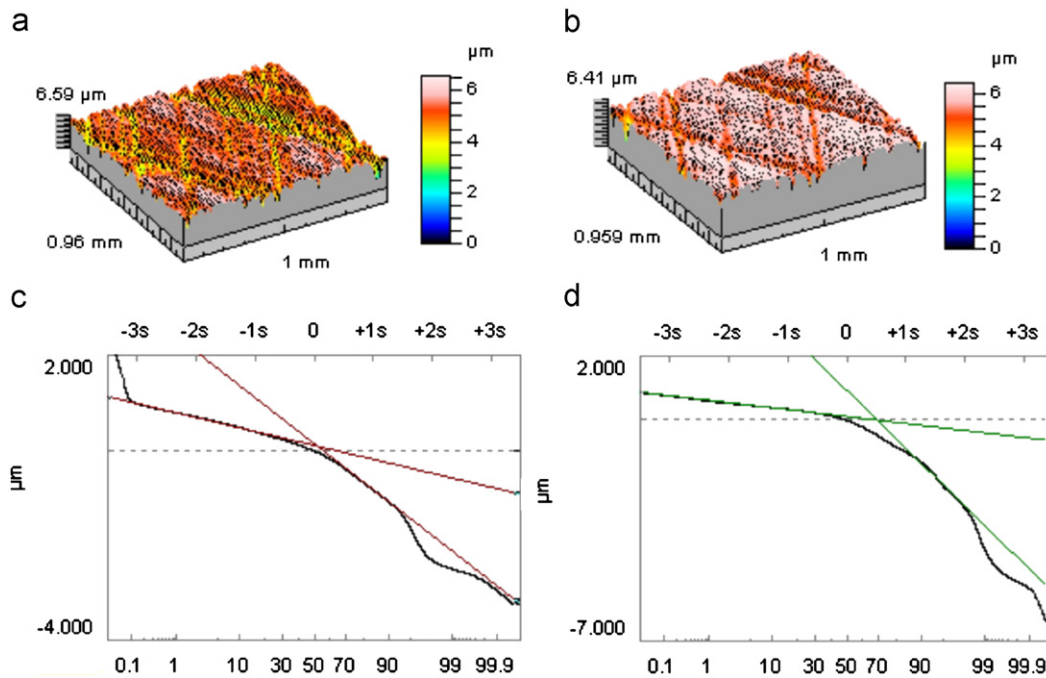


Fig. 15. Contour plots of surface details (a, b) and probability plots of material ratio curve (c, d) of II-0.7 sample before (a, c) and after test (b, d).

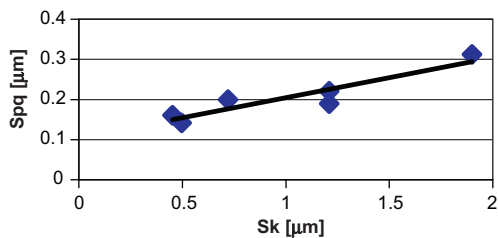


Fig. 16. Dependence between  $Sk$  and  $Spq$  parameters of worn two-process surfaces.

the necessity of further modification of the tribological tester. The values of the coefficient of friction usually decreased during wear process.

- (3) It is possible to obtain information about local linear wear values based only on worn surface measurement. The analysis of changes of 3D surface parameters is another possibility. We recommend use of decreases in the  $Sk$  parameter as a linear wear measure.
- (4) During the “zero-wear” process a two-process structure is created. The characteristic feature of the wear process is a decrease of skewness  $Ssk$ , increase of kurtosis  $Sku$  and of the spatial parameter  $Sal$ . Amplitude parameters characterising the peak surface part  $Sp$ ,  $Spk$  and core decreased. The greatest changes took place in the parameters  $Ssc$  and  $Sbi$ . The largest parameters (especially describing the peak surface part) changes were noticed after 0.5–1 h of operating.

## References

- [1] Sudarshan TS, Bhadun SB. Wear in cylinder liner. *Wear* 1983;91:269–77.
- [2] Wiemann L. Die Bildung von Brandspuren auf den Laufflächen der Paarung Kolbenring-Zylinder in Verbrennungsmotoren. *Motortechnische Z* 1971; 32(2):43–9.
- [3] Haynes GP, Hyde GF, Sauter GW, Thornton TE. Accelerated chromium plate piston ring wear associated with line pitting. SAE paper 1983; 831280.
- [4] Sreenath AV, Raman N. Running-in wear of a compression ignition engine: factors influencing the conformance between cylinder liner and piston rings. *Wear* 1976;38:271–89.
- [5] Campbell JC. Cylinder bore surface roughness in internal combustion engines: its appreciation and control. *Wear* 1972;19:163–8.
- [6] Pawlus P. A study on the functional properties of honed cylinder surface during running-in. *Wear* 1994;176:247–54.
- [7] Pawlus P. Effects of honed cylinder surface topography on the wear of piston-piston ring-cylinder assemblies under artificially increased dustiness conditions. *Tribology International* 1993;26(1):49–55.
- [8] Tomanik E. Friction and wear bench tests of different engine liner surface finishes. *Tribology International* 2008;41:1032–8.
- [9] Bigerelle M, Hagege B, El Mansori M. Mechanical modeling of micro-scale abrasion in superfinish belt grinding. *Tribology International* 2008;41: 992–1001.
- [10] Jeng Y. Impact of plateaued surfaces on tribological performance. *Tribology Transactions* 1996;39(2):354–61.
- [11] Almsyah C, Dillich S, Pettit A. The effect of surface finish on cam wear. *Wear* 1989;134:29–47.
- [12] Kumar R, Prakash B, Sethuramiah A. A systematic methodology to characterise the running-in and steady-state wear process. *Wear* 2002;252: 445–53.
- [13] Masouros G, Dimaragonas A, Lefas K. A model for wear and surface roughness transient during the running-in of bearings. *Wear* 1977;45:375–83.
- [14] Rosen B-G, Ohlsson R, Thomas TR. Tribological implications of AFM measurements of cylinder bore microtopography. In: Proceedings of the conference on atomic scale control of surfaces and interfaces, Brighton, UK; 1994.
- [15] Daskivich RA. Bearing length ratio applied to the measurement of engine cylinder-bore wear. *Precision Engineering* 1984;6:31–3.
- [16] Pawlus P. A method of measuring “zero-wear” of the cylinder liner. *Tribotest* 1998;5(1):53–70.
- [17] Kumar RS, Prakash B, Sethuramiah A. Assessment of engine liner wear from bearing area curves. *Wear* 2000;239:282–6.
- [18] Johansson S, Nilsson PH, Ohlsson R, Anderberg C, Rosen B-G. New cylinder liner surfaces for low oil consumption. *Tribology International* 2008;41: 854–9.
- [19] Gahlén R, Jacobson S. A novel method to map and quantify wear on a micro-scale. *Wear* 1998;222:93–100.
- [20] Sasajima K, Naoi K, Tsukada T. A software-based relocation technique for surface asperity profiles and its application to calculate volume changes in running-in wear. *Wear* 2000;240:152–61.
- [21] Condeco J, Christensen LH, Rosen B-G. Software relocation of 3D surface topography measurements. In: Proceedings of the 8th international conference on metrology & properties of engineering surfaces. Huddersfield, UK; 2000. p. 203–8.

- [22] Stout KJ, Sullivan PJ, Dong WP, Mainsah E, Luo N, Mathia T, et al. The development of methods for the characterisation of roughness in three dimensions. Publication EUR 15178 EN Commission of the European Communities; 1993.
- [23] Pawlus P, Grabon W. Description of multi-process surface topography. In: Proceedings of the 12th international conference on metrology and properties of engineering surfaces, Rzeszow, Poland; 2009. p. 301–6.
- [24] Pawlus P, Galda L, Dzierwa A, Koszela W. Abrasive wear resistance of textured steel rings. *Wear* 2009;267:1873–82.
- [25] Pawlus P. Characterisation of low wear of engine parts. *Finnish Journal of Tribology (TRIBOLOGIA)* 2007;26(2):10–24.